

RESEARCH

Open Access



# Sequential pretreatment with hydroxyl radical and manganese peroxidase for the efficient enzymatic saccharification of corn stover

Man Zhou<sup>1</sup>, Yaru Wang<sup>1</sup>, Yuan Wang<sup>1</sup>, Tao Tu<sup>1</sup>, Jie Zhang<sup>1</sup>, Xiaolu Wang<sup>1</sup>, Guijie Zhang<sup>2</sup>, Huoqing Huang<sup>1</sup>, Bin Yao<sup>1</sup>, Huiying Luo<sup>1\*</sup> and Xing Qin<sup>1\*</sup>

## Abstract

**Background** White rot fungi produce various reactive oxygen species and ligninolytic enzymes for lignocellulose deconstruction. However, their interactions during the deconstruction of lignocellulosic structural barriers for efficient enzymatic saccharification remain unclear.

**Results** Herein, the extracellular enzyme activities and secretomic analysis revealed the sequential expression of hydroxyl radical ( $\cdot\text{OH}$ ) and manganese peroxidases (MnPs) for lignocellulose deconstruction by the white rot fungus *Irpex lacteus*. Subsequently, in vitro functional studies found that  $\cdot\text{OH}$  possessed the ability to disrupt the smooth surface structure of corn stover, resulting in increased enzymatic saccharification and cellulose accessibility. Purified recombinant MnPs from *I. lacteus* were able to cleave the  $\beta\text{-O-4}$  bond in phenolic and non-phenolic lignin model dimers without the help of any mediators. Furthermore, the sequential pretreatment of corn stover with  $\cdot\text{OH}$  and MnP exhibited significant synergistic effects, increasing enzymatic saccharification and cellulose accessibility by 2.9-fold and 1.8-fold, respectively.

**Conclusions** These results proved for the first time the synergistic effects of  $\cdot\text{OH}$  and MnP pretreatment in improving the enzymatic saccharification and cellulose accessibility of corn stover. These findings also demonstrated the potential application of  $\cdot\text{OH}$  and MnP pretreatment for the efficient enzymatic saccharification of corn stover.

**Keywords** Hydroxyl radical, Manganese peroxidase, Pretreatment, Enzymatic saccharification, Corn stover

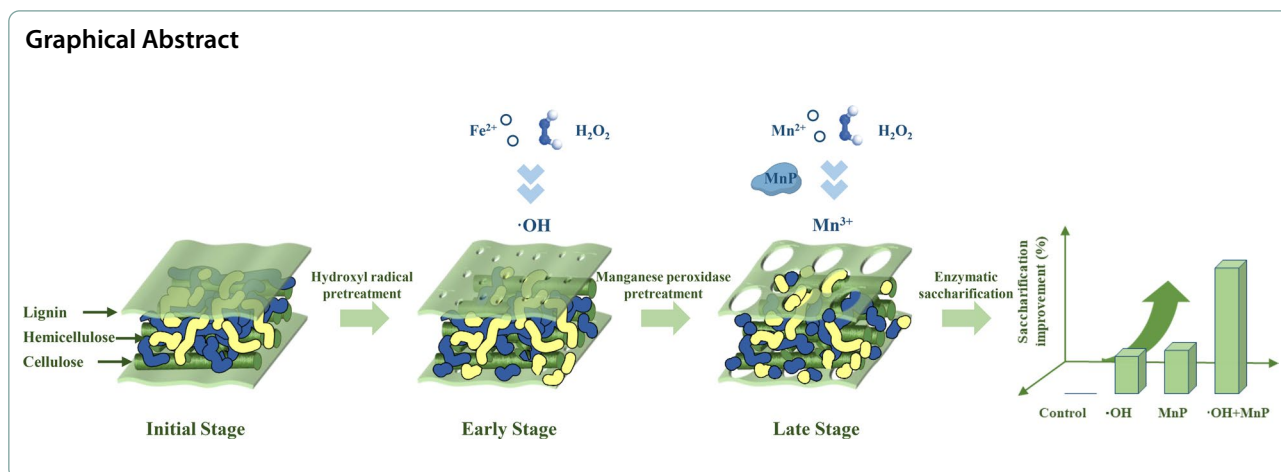
\*Correspondence:

Huiying Luo  
luohuiying@caas.cn  
Xing Qin  
qinxing@caas.cn

Full list of author information is available at the end of the article



© The Author(s) 2024. **Open Access** This article is licensed under a Creative Commons Attribution-NonCommercial-NoDerivatives 4.0 International License, which permits any non-commercial use, sharing, distribution and reproduction in any medium or format, as long as you give appropriate credit to the original author(s) and the source, provide a link to the Creative Commons licence, and indicate if you modified the licensed material. You do not have permission under this licence to share adapted material derived from this article or parts of it. The images or other third party material in this article are included in the article's Creative Commons licence, unless indicated otherwise in a credit line to the material. If material is not included in the article's Creative Commons licence and your intended use is not permitted by statutory regulation or exceeds the permitted use, you will need to obtain permission directly from the copyright holder. To view a copy of this licence, visit <http://creativecommons.org/licenses/by-nc-nd/4.0/>.



## Background

Lignocellulosic biomass, as a renewable resource that is widely available and abundant, offers a promising alternative feedstock for the manufacturing of bio-based products, without affecting the food supply [1, 2]. However, the recalcitrant structure of lignocellulosic biomass, in particular the lignin barrier structure, poses a huge challenge for efficient enzymatic saccharification to convert the polysaccharide composition into simple sugars that can be directly utilized for bio-based biorefineries [3, 4]. Nonetheless, certain fungal species in nature, such as white rot fungi, have evolved the remarkable ability to selectively degrade the lignin component, leaving behind the polysaccharide composition [5–7], showing great potential in breaking down the recalcitrant structure of lignocellulosic biomass. Thus, an in-depth understanding of the unique degradation machinery of white rot fungi would be beneficial for achieving the efficient enzymatic saccharification of lignocellulosic biomass.

As reported, white rot fungi produce various types of reactive oxygen species and ligninolytic enzymes to break down structural barriers in lignocellulosic biomass [8, 9]. Given the limited surface area of lignocellulosic biomass available for ligninolytic enzymes interaction, it has been postulated that reactive oxygen species play an important role in the initial stage of structural barriers degradation [8, 10]. For example, hydroxyl radical ( $\cdot\text{OH}$ ), the most common reactive oxygen species in white rot fungi, indiscriminately attacks all structural components of lignocellulosic biomass, resulting in cleavages that allow the penetration of ligninolytic enzymes [11]. However, it is worth noting that  $\cdot\text{OH}$  could also cause conformational changes and structural decomposition of lignocellulosic biomass, leading to inhibition of their enzymatic activity or enzyme inactivation [12, 13]. As a consequence, identifying and elucidating the relationship between the

generation of reactive oxygen species and the production and activity of ligninolytic enzymes in white rot fungi could provide valuable insights for advancing the field of lignocellulosic biomass pretreatment.

During the biological pretreatment of lignocellulosic biomass by white rot fungi, sequential expression patterns of reactive oxygen species and ligninolytic enzymes have been found in previous studies [14–16]. At the early stages of lignocellulosic biomass degradation,  $\text{Fe}^{3+}$ -reducing capability, related to the generation of  $\cdot\text{OH}$ , occurs prior to the production of ligninolytic enzymes, and rapidly reaches a maximum and then decreases. Subsequently, ligninolytic enzymes, in particular the class II manganese peroxidase (MnP), appear and quickly rise to peak levels. Although these phenomena have been observed, the underlying synergistic mechanism between reactive oxygen species and ligninolytic enzymes in breaking down structural barriers to facilitate the efficient enzymatic saccharification of lignocellulosic biomass needs to be further investigated.

*Irpex lacteus* is one of the most potent lignocellulose biomass biological pretreated white rot fungi, capable of selectively degrading the lignin component in agricultural biomass, such as corn stover and wheat straw [17–19]. Based on the genome analysis of reported *I. lacteus* strains in the JGI database, it was found that they are equipped with a comprehensive set of ligninolytic enzymes, mainly including MnP, versatile peroxidases, lignin peroxidases, and dye-decolorizing peroxidases [20]. In addition, the sequential generation of reactive oxygen species and ligninolytic enzymes in *I. lacteus* during the degradation of corn stover was found in our previous study [14]. However, the mechanism underlying the interaction between reactive oxygen species and ligninolytic enzymes in the breakdown of structural barriers for efficient enzymatic saccharification of corn stover remains unclear.

In this study, extracellular enzyme activities and temporal secretomic analysis of *I. lacteus* 7B growth on corn stover were performed to reveal the composition of reactive oxygen species and ligninolytic enzymes in *I. lacteus* during lignocellulosic biomass degradation. Subsequently, the effect of reactive oxygen species ( $\cdot\text{OH}$ ) on the breakdown of structural barriers in corn stover and the function of the core ligninolytic enzymes MnPs in the depolymerization of lignin model dimers guaiacylglycerol- $\beta$ -guaiacyl ether (GBG) and veratrylglycerol- $\beta$ -guaiacyl ether (VBG) were investigated in vitro. Based on this, the sequential pretreatment with  $\cdot\text{OH}$  and MnP for the efficient enzymatic saccharification of corn stover was further evaluated.

## Materials and methods

### Strains and culture conditions

The mononucleate strain *I. lacteus* 7B, which was isolated from *I. lacteus* CGMCC 5.809 purchased from the China General Microbiological Culture Collection Center, was cultured in potato dextrose broth medium for seven days. Subsequently, it was inoculated into modified Kirk's medium supplemented with 1% (w/v) corn stover as the sole carbon source for lignocellulosic biomass degradation at 30 °C and 150 rpm. *Escherichia coli* BL21 (DE3) and the corresponding expression vector pET28a were obtained from TransGen Biotech and Invitrogen, respectively.

### Determination of reactive oxygen species generating capacity and ligninolytic enzyme activities

Iron-reducing capability was assessed by measuring the formation of the  $\text{Fe}^{2+}$ -ferrozine complex in pH 5.0 acetate buffer containing 4 mM ferrozine and 0.3 mM  $\text{FeCl}_3$  [21]. One unit of iron-reducing activity was defined as the increase in absorbance at 562 nm per minute. The ability of generating  $\text{H}_2\text{O}_2$  was determined by monitoring the generation of resorufin according to the Amplex Red Hydrogen Peroxide/Peroxidase Assay Kit purchased from ThermoFisher [22]. One unit of  $\text{H}_2\text{O}_2$ -generating activity was defined as the amount of enzyme generating 1  $\mu\text{mol}$   $\text{H}_2\text{O}_2$  per minute. Total ligninolytic peroxidase activity was measured by observing the oxidation of 2,2'-azino-bis(3-ethylbenzothiazoline-6-sulphonic acid) (ABTS) at 420 nm in pH 4.0 malonate buffer containing 1 mM ABTS, 1 mM  $\text{MnSO}_4$ , and 0.1 mM  $\text{H}_2\text{O}_2$ . MnP activity was measured by monitoring the oxidation of  $\text{MnSO}_4$  at 270 nm in pH 4.0 malonate buffer containing 1 mM  $\text{MnSO}_4$  and 0.1 mM  $\text{H}_2\text{O}_2$ . One unit of total ligninolytic peroxidase and MnP activity was defined as the amount

of enzyme oxidizing 1  $\mu\text{mol}$  of the corresponding substrate per minute.

### Temporal secretomic analysis of *I. lacteus* 7B growth on corn stover

The supernatant of *I. lacteus* 7B growth in modified Kirk's medium supplemented with 1% (w/v) corn stover on days 1, 2, and 3 was collected and sent to Allwegene Technology for temporal secretomic analysis. Established protocols were followed for total protein extraction, protein quality testing, trypsin treatment, and nano-HPLC-MS/MS analysis of protein samples [23]. Subsequently, the MaxQuant software was used to process and quantify the MS/MS data in accordance with the *I. lacteus* 7B protein database [24]. The following analytical parameters were configured: trypsin was used as the enzyme, with a maximum of two missed cleavage sites allowed; an MS/MS tolerance of 20 ppm was set; and variable and fixed modifications were oxidation (M) and carbamidomethyl (C), respectively.

### Effect of reactive oxygen species ( $\cdot\text{OH}$ ) on the breakdown of structural barriers in corn stover

The  $\cdot\text{OH}$  pretreatment of corn stover was conducted in vitro using a biomimetic system with various concentrations of  $\text{FeSO}_4$  (0–40 mM) and  $\text{H}_2\text{O}_2$  (0–2 M). The reaction was carried out with 10% (w/v) corn stover at 25 °C and 200 rpm for 24 h. After the reaction, the pretreated corn stover was centrifuged, washed, dried, and subjected to enzymatic saccharification. Enzymatic saccharification was performed in pH 5.0 acetate buffer using commercial cellulase (SAE0020, purchased from Sigma-Aldrich) at 40 FPU/g substrate and 0.5% (w/v) pretreated corn stover at 30 °C with agitation at 1000 rpm for 24 h. The generated reducing sugars were quantified using the 3,5-dinitrosalicylic acid assay [25]. Meanwhile, scanning electron microscopy (SEM) SU8010 (Hitachi, Japan) was used to analyze the surface morphological characteristics of corn stover after pretreatment with  $\cdot\text{OH}$ . Prior to microscopic analysis, the pretreated corn stover was adhered to a copper plate using a black adhesive tape and then coated with gold.

### Effect of the core ligninolytic enzymes MnPs in the depolymerization of lignin model dimers

The cDNA fragments of the core ligninolytic enzymes MnPs were cloned and assembled into the expression vector pET28a to obtain recombinant plasmids pET28a-*lMnP1*, pET28a-*lMnP2*, and pET28a-*lMnP4*, which were then transformed into the expression host *E. coli* BL21 (DE3) individually. The specific primers used are listed in Additional file 1. The induction of expression,

refolding, and purification of the recombinant MnPs were carried out according to the protocols described previously [21]. The purified recombinant MnPs were firstly analyzed by UV-vis spectroscopy in the range of 230–900 nm to verify the correct incorporation of heme groups. Subsequently, the substrate specificities of MnPs were investigated for the oxidation of six different substrates, including ABTS, 2,6-dimethylphenol (DMP), guaiacol (GUA),  $\text{Mn}^{2+}$ , reactive black 5 (RB5), reactive black 19 (RB19).

The ability of MnPs to depolymerize the lignin barrier structure was evaluated by degrading the phenolic and non-phenolic lignin model dimers, GBG and VBG. The degradation of GBG/VBG was initiated in pH 4.0 malonate buffer containing 1 mM GBG/VBG, 1 mM  $\text{MnSO}_4$ , 0.1 mM  $\text{H}_2\text{O}_2$ , and 1 U/mL MnP (ABTS as substrate). The reaction was supplemented with 0.1 mM  $\text{H}_2\text{O}_2$  every 12 h and 1 U/mL MnP every 24 h and continued at 30 °C for 72 h. Samples were collected at 12, 24, 48, 60, and 72 h, and analyzed for degradation ratio using HPLC with a Hypersil GOLD™ C18 column at 280 nm and a flow rate of 0.6 mL/min. The elution condition was gradient elution of mobile phase A (methanol) and mobile phase B (0.1% acetic acid) for 10% A, 27 min; 40% A, 33 min; 44% A, 10 min; and 10% A, 10 min. To confirm the oxidation product of GBG/VBG, UPLC-MS/MS analysis was carried out using a Nexera UHPLC system coupled to an AB-SCIEX 5600 Triple TOF mass spectrometer. The ion source gases GS1, GS2, and curtain gas were adjusted to 60, 60, and 40 psi, respectively. In addition, the temperature and ion spray voltage floating were set at 600 °C and 5500 V, respectively.

#### Effect of sequential pretreatment with $\cdot\text{OH}$ and MnP on the enzymatic saccharification of corn stover

First, the pretreatment of corn stover with  $\cdot\text{OH}$  was carried out using 10% (w/v) corn stover, 20 mM  $\text{FeSO}_4$ , and 1 M  $\text{H}_2\text{O}_2$ . The reaction was performed at 200 rpm and 25 °C for 24 h. Subsequently, the pretreated corn stover was centrifuged, washed, and dried. Then, the pretreatment of  $\cdot\text{OH}$  pretreated corn stover with MnP was conducted in pH 4.0 malonate buffer containing 10% (w/v)  $\cdot\text{OH}$  pretreated corn stover, 1 mM  $\text{MnSO}_4$ , 0.1 mM  $\text{H}_2\text{O}_2$ , and 1 U/mL *l*MnP1. The reaction was continued at 30 °C for 72 h, and 0.1 mM  $\text{H}_2\text{O}_2$  and 1 U/mL *l*MnP1 were supplemented every 12 h and 24 h, respectively. After that, the resulting pretreated corn stover was centrifuged, washed, and dried for enzymatic saccharification. Enzymatic saccharification was performed in pH 5.0 acetate buffer using commercial cellulase at 40 FPU/g substrate and 0.5% (w/v) pretreated corn stover at 30 °C with agitation at 1000 rpm for 24 h. Control groups were set up by pretreating corn stover individually with  $\cdot\text{OH}$

or MnP. Synergistic effects were assessed as the ratio of the improvement in reducing sugars production in the sequential pretreatment group divided by the sum of the improvements in reducing sugars production in the individual pretreatment groups.

Meanwhile, the variations in cellulose accessibility of corn stover after the sequential pretreatment with  $\cdot\text{OH}$  and MnP were assessed semi-quantitatively using the dyes Direct Orange 15 (DO15) and Direct Blue 1 (DB1) [26, 27]. Specifically, 100 mg of corn stover were combined with 1 mL phosphate buffer containing 1.4 M NaCl and varying volumes of the DO15/DB1 mixture, resulting in final dye concentrations ranged from 0.025 to 0.8 mg/mL. Next, the samples were diluted ten times and incubated at 70 °C for 6 h. After incubation, the absorbance of DO15 and DB1 in the supernatant was measured at 455 nm and 624 nm, respectively. The dye content was determined using established absorbance-concentration standard curves. Based on this, the adsorption capacities of DO15 and DB1 were calculated using the Langmuir isotherm adsorption model based on the total amount of dye added [27].

## Results and discussion

### Extracellular enzyme activities and temporal secretomic analysis revealed reactive oxygen species and ligninolytic enzymes involved in lignocellulose deconstruction by *I. lacteus* 7B

In order to confirm whether reactive oxygen species and ligninolytic enzymes were involved in the breakdown of structural barriers in corn stover by *I. lacteus* 7B, the corresponding extracellular activities in the supernatant were preferentially determined. With regard to reactive oxygen species, a high iron-reducing activity was found in the supernatant on day 1 and decreased with time (Fig. 1A). In addition,  $\text{H}_2\text{O}_2$ -generating activity was also observed throughout the whole degradation process (Fig. 1B), suggesting that  $\cdot\text{OH}$  generated by the Fenton reaction ( $\text{Fe}^{2+}/\text{H}_2\text{O}_2$ ) might participate in the degradation of corn stover. As for the ligninolytic enzymes, the total ligninolytic peroxidase and MnP activities of the supernatant reached the similar peak value on day 2 (Fig. 1C and D), corresponding to 46.95 and 40.89 U/L, respectively. Furthermore, no lignin peroxidase activity was detected using veratryl alcohol as a substrate, revealing that MnPs could be the core ligninolytic enzymes responsible for the breakdown of the lignin barrier structure. Taken together, these extracellular activity results indicated that  $\cdot\text{OH}$ -derived reactive oxygen species and the MnP-centered ligninolytic enzyme might be involved in the deconstruction of lignocellulosic structural barriers by *I. lacteus* 7B.

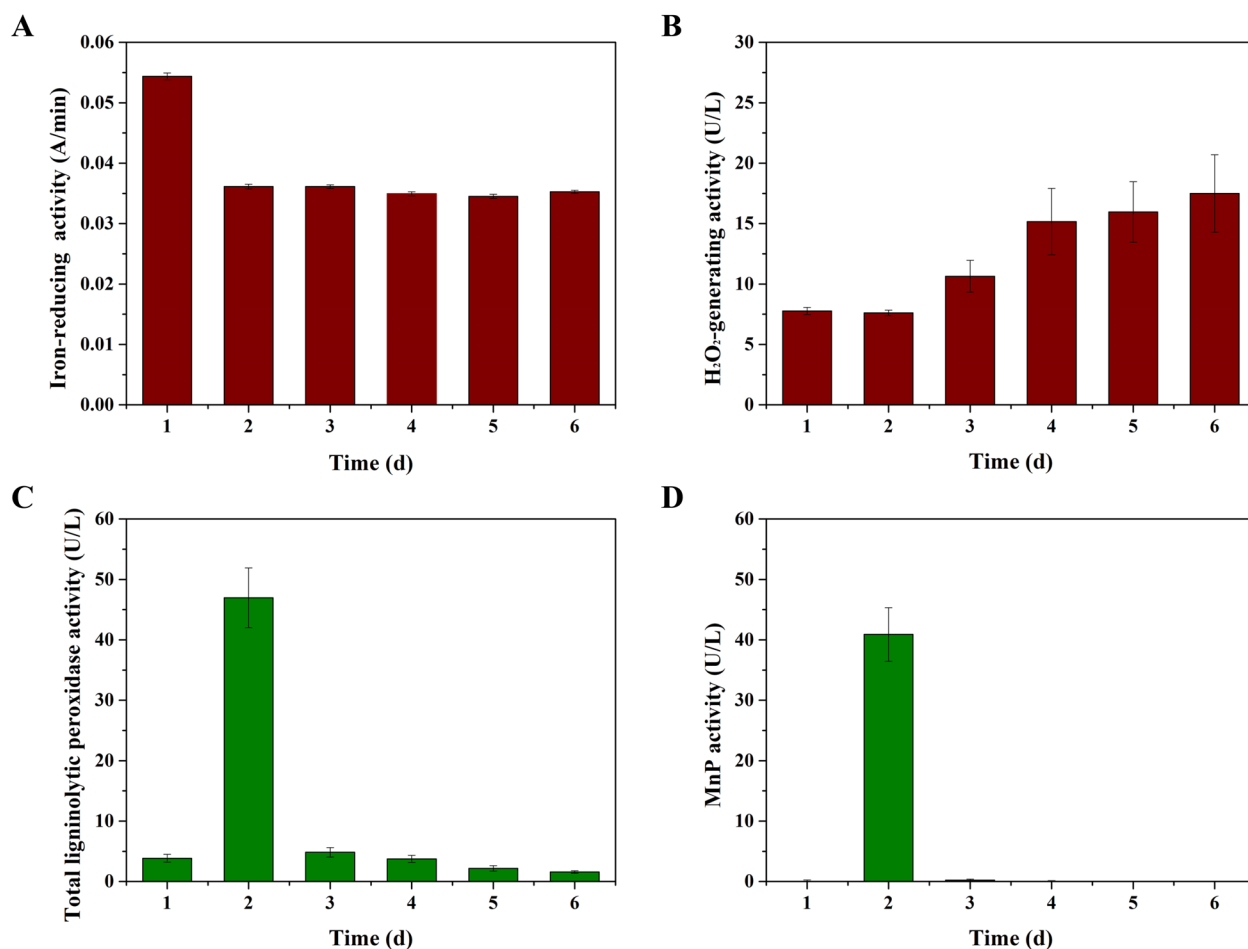


**Fig. 1** Time course analysis of extracellular reactive oxygen species generating capacity and ligninolytic enzyme activities of *I. lacteus* 7B growth on corn stover. Iron-reducing activity (A), H<sub>2</sub>O<sub>2</sub>-generating activity (B), total ligninolytic peroxidase activity (C), and MnP activity (D)

Considering the diversity of ligninolytic enzymes in white rot fungi, temporal secretomic analysis of the supernatants of *I. lacteus* 7B cultured on corn stover for 1, 2, and 3 days was performed to further investigate the composition of the ligninolytic enzymes in *I. lacteus*. As shown in Fig. 2A, the expression profile of ligninolytic enzymes consisted of multiple ligninolytic peroxidases, including six MnPs (*IIMn*P1, *IIMn*P2, *IIMn*P3, *IIMn*P4, *IIMn*P5, and *IIMn*P6), three dye-decolorizing peroxidases, and one lignin peroxidase. Remarkably, the expression level of MnPs except *IIMn*P6 on day 2 was 10–1000 times higher than that of other ligninolytic peroxidases. This was consistent with the extracellular enzyme activities of the total ligninolytic peroxidase and MnP. No lignin peroxidase was detected in the supernatant, which might be due to low expression levels. In addition, various H<sub>2</sub>O<sub>2</sub>-generating auxiliary enzymes were also found in the supernatants throughout the whole degradation process, including

alcohol oxidase, pyranose oxidase, cellobiose dehydrogenase, glyoxal oxidase, gluco-oligosaccharide oxidase, and lytic polysaccharide monooxygenase (Fig. 2B), which could generate H<sub>2</sub>O<sub>2</sub> using aromatic compounds from lignin degradation or oligosaccharides from polysaccharide depolymerization as substrates [28].

Based on the above extracellular enzyme activities and secretomic analysis, it could be concluded that *I. lacteus*, like other reported white rot fungi, produced extracellular reactive oxygen species, but also secreted ligninolytic enzymes involved in the degradation of lignocellulosic structural barriers [8, 9]. However, the individual and combined effects of ·OH and MnP pretreatment on the enzymatic saccharification of corn stover remained unclear. In recent years, in vitro mimicking ·OH pretreatment of lignocellulosic biomass, including corn stover, wheat straw, and rice straw, had been gradually carried out to evaluate its effect on enzymatic saccharification efficiency [29, 30]. According to the results of enzymatic

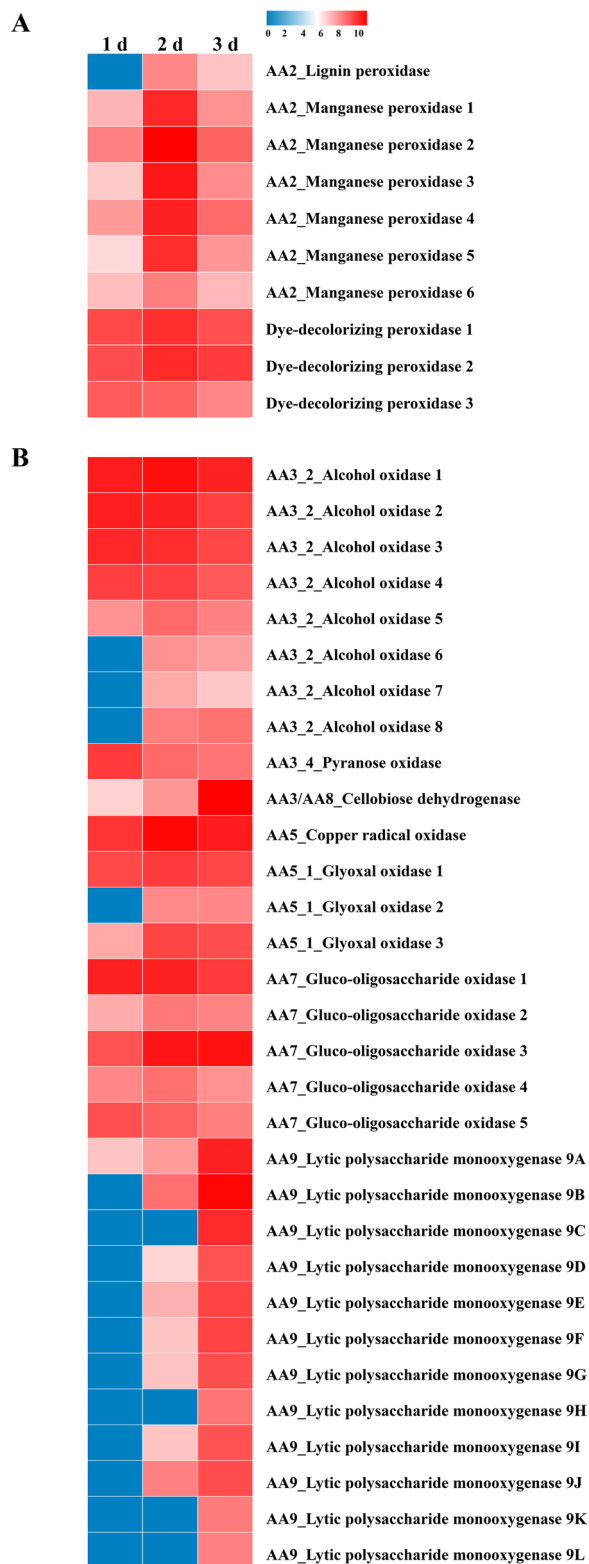


**Fig. 2** Protein abundance of ligninolytic enzymes (A) and H<sub>2</sub>O<sub>2</sub>-generating auxiliary enzymes (B) in the secretome of *I. lacteus* 7B growth on corn stover for 1, 2, and 3 days. Heatmaps were constructed based on the log<sub>10</sub>-transformed protein LFQ-based intensity values

saccharification and structural composition determination, it was found that ·OH pretreatment resulted in improved glucose production due to increased cellulose accessibility rather than lignin degradation [29]. Meanwhile, the function of ligninolytic enzymes, particularly laccases, in removing the lignin component of lignocellulosic biomass in vitro had also been demonstrated, but the effect on the enzymatic saccharification of lignocellulosic biomass after pretreatment remained ambiguous due to the inhibition of ligninolytic enzymes or their degradation products on cellulase activity and cellulose hydrolysis [31, 32]. Although these phenomena had been observed, the combined effect of ·OH and MnP pretreatment on the enzymatic saccharification of lignocellulosic biomass remained to be further investigated.

**Effect of ·OH generated by the Fenton reaction on the breakdown of structural barriers in corn stover**

To evaluate the impact of ·OH pretreatment on the breakdown of structural barriers in corn stover, an in vitro ·OH generation system based on the Fenton reaction was initially established and subsequently employed to pretreat corn stover. In regard to the ·OH generation system, the different concentrations of Fenton reagents (Fe<sup>2+</sup> and H<sub>2</sub>O<sub>2</sub>) utilized in the pretreatment of corn stover was assessed, as the generation of ·OH was closely correlated to the concentration of Fenton reagents [33, 34]. As shown in Fig. 3, the increase in FeSO<sub>4</sub> concentration resulted in a noticeable enhancement in the release of reducing sugars during the enzymatic saccharification of the pretreated corn stover. The maximum production of reducing sugars was achieved at a concentration of 20 mM FeSO<sub>4</sub> (Fig. 3A). Likewise, a rise in H<sub>2</sub>O<sub>2</sub> concentration also led to a proportional increase in reducing sugars production, with the maximum production observed at a concentration of 1 M H<sub>2</sub>O<sub>2</sub> (Fig. 3B). Thus, 20 mM FeSO<sub>4</sub> and 1 M H<sub>2</sub>O<sub>2</sub> were used to generate ·OH in vitro through the Fenton reaction. After 24 h ·OH pretreatment, the reducing sugars production reached 0.32 mg/mL after enzymatic saccharification of pretreated corn stover using commercial cellulase, while the control without pretreatment was 0.16 mg/mL (Fig. 3C).

Meanwhile, the changes in the surface structure of corn stover after ·OH pretreatment were observed by SEM analysis (Fig. 4). While pretreatment with 20 mM FeSO<sub>4</sub> or 1 M H<sub>2</sub>O<sub>2</sub> alone did not significantly alter the

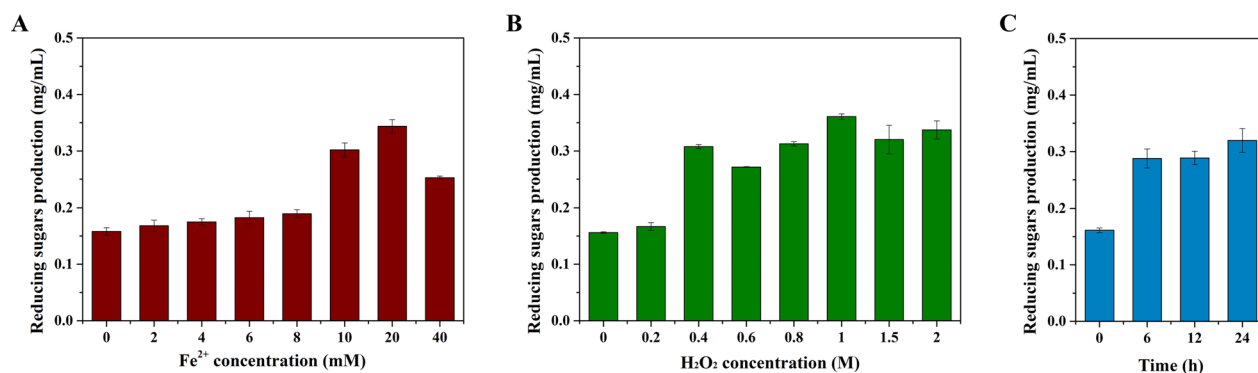


**Fig. 3** Effects of  $\cdot\text{OH}$  generated by the Fenton reaction pretreatment on the enzymatic saccharification of corn stover. Effect of  $\text{Fe}^{2+}$  concentration in the presence of 1 M  $\text{H}_2\text{O}_2$  (A),  $\text{H}_2\text{O}_2$  concentration in the presence of 20 mM  $\text{FeSO}_4$  (B), and pretreatment time on reducing sugars production in the presence of 20 mM  $\text{FeSO}_4$  and 1 M  $\text{H}_2\text{O}_2$  (C)

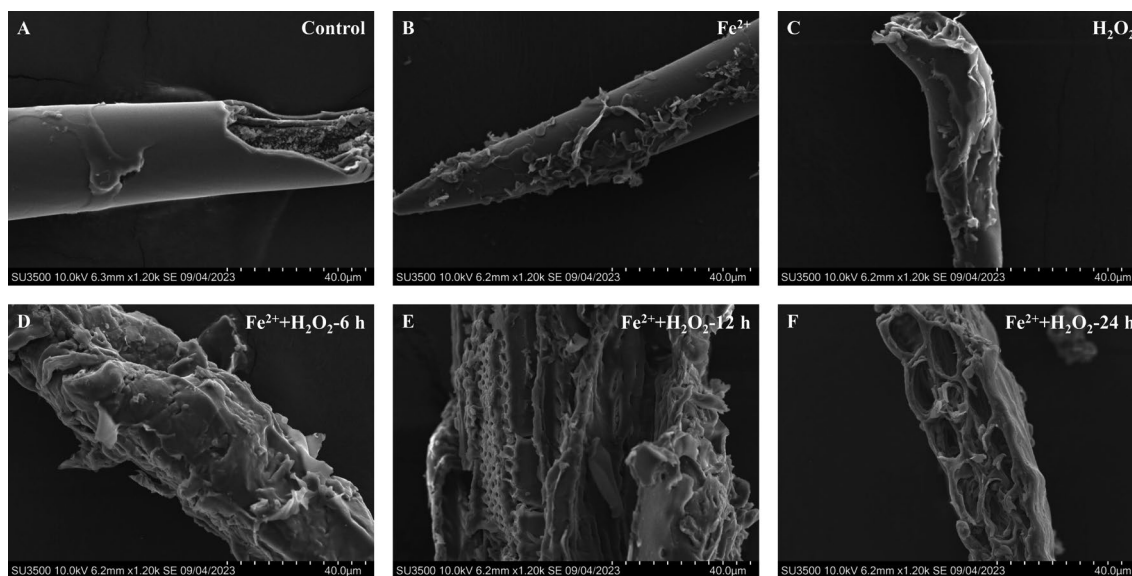


**Fig. 4** Scanning electron microscopic analysis of corn stover after  $\cdot\text{OH}$  pretreatment. Control (A),  $\text{Fe}^{2+}$  pretreatment alone for 24 h (B),  $\text{H}_2\text{O}_2$  pretreatment alone for 24 h (C), and  $\text{Fe}^{2+}$  plus  $\text{H}_2\text{O}_2$  pretreatment for 6, 12, and 24 h (D–F)

surface structure of corn stover compared to the control group without chemical pretreatment, the application of 20 mM  $\text{FeSO}_4$  and 1 M  $\text{H}_2\text{O}_2$  resulted in pronounced morphological changes. As the pretreatment time was increased, the outer layers of the corn stover were progressively stripped away, revealing an increasing number of small openings which subsequently expanded to expose the underlying cellulose. This erosion might increase the contact surface between the cellulolytic enzymes and the internal cellulose, potentially enhancing the efficiency of enzymatic saccharification in corn stover [35].

Combining enzymatic saccharification and SEM analysis of  $\cdot\text{OH}$  pretreated corn stover, it was found

that  $\cdot\text{OH}$  pretreatment could significantly enhance the enzymatic hydrolysis of corn stover through breaking down lignocellulosic structural barriers, confirming the biological function of  $\cdot\text{OH}$  for the efficient enzymatic saccharification of lignocellulosic biomass. Most notably, after  $\cdot\text{OH}$  pretreatment, the smooth surface structure of the corn stover was severely damaged and produced a large number of small openings. As a result, the cellulose accessibility of  $\cdot\text{OH}$  pretreated corn stover to cellulolytic enzymes increased significantly (Fig. 7B), resulting in an increase in reducing sugars production during enzymatic saccharification. This phenomenon was consistent with previous reports [29, 30]. Although this structural change allowed increased infiltration

of cellulolytic enzymes for efficient enzymatic saccharification of corn stover, it remained to be explored whether this would favor the subsequent action of the ligninolytic enzyme MnP in the pretreatment of corn stover.

### Effect of the core ligninolytic enzyme MnP on lignin depolymerization

To elucidate the function of the core ligninolytic enzyme MnP in the depolymerization of the lignin barrier structure in lignocellulosic biomass, three highly expressed MnPs (*II*MnP1, *II*MnP2, and *II*MnP4) were selected for heterologous recombinant expression in *E. coli* and then purified to evaluate their function. As shown in Additional file 2, three MnPs were successfully expressed and refolded into the active form, based on the identification of the characteristic absorption spectra of heme groups through UV-vis spectroscopy analysis. These purified recombinant MnPs demonstrated a broad substrate specificity, encompassing the model ligninolytic enzyme substrate ABTS, the typical manganese peroxidase substrate  $Mn^{2+}$ , aromatic compounds such as DMP and GUA, and the dyes RB5 and RB19 (Additional file 3). In addition, three MnPs exhibited an optimum pH of 4.0 for these four types of substrates.

Subsequently, the  $\beta$ -O-4 phenolic and non-phenolic lignin model dimers GBG and VBG were used as substrates to evaluate the lignin depolymerization ability of the MnPs. As shown in Fig. 5, these purified recombinant *II*MnP1, *II*MnP2, and *II*MnP4 showed a remarkable capacity for degrading GBG and VBG. Besides, the addition of MnP and  $H_2O_2$  in a continuous manner led to the attainment of the highest degradation ratios of both GBG and VBG. Specifically, the degradation ratio for GBG reached 61.79%, 60.14%, and 61.04% at 72 h for *II*MnP1, *II*MnP2, and *II*MnP4, respectively. In comparison to the  $\beta$ -O-4 phenolic lignin model dimer GBG, the degradation ratio of the non-phenolic lignin model dimer VBG by MnPs exhibited a certain decrease. The degradation ratios for VBG were found to be 51.42%, 42.64%, and 42.71% at 72 h for *II*MnP1, *II*MnP2, and *II*MnP4, respectively.

In the meantime, to further confirm the occurrence of lignin inter-unit bond cleavage, UPLC-MS/MS analysis was conducted to identify the degradation products of GBG and VBG by MnPs (Additional file 4). For the oxidation products of GBG, the main reaction products identified were compound I ( $C_{17}H_{18}O_6$ ) and compound II ( $C_{10}H_{12}O_4$ ). On the other hand, the oxidized compound III ( $C_{18}H_{20}O_6$ ) and compound IV ( $C_{11}H_{14}O_4$ ) were observed in the oxidation products

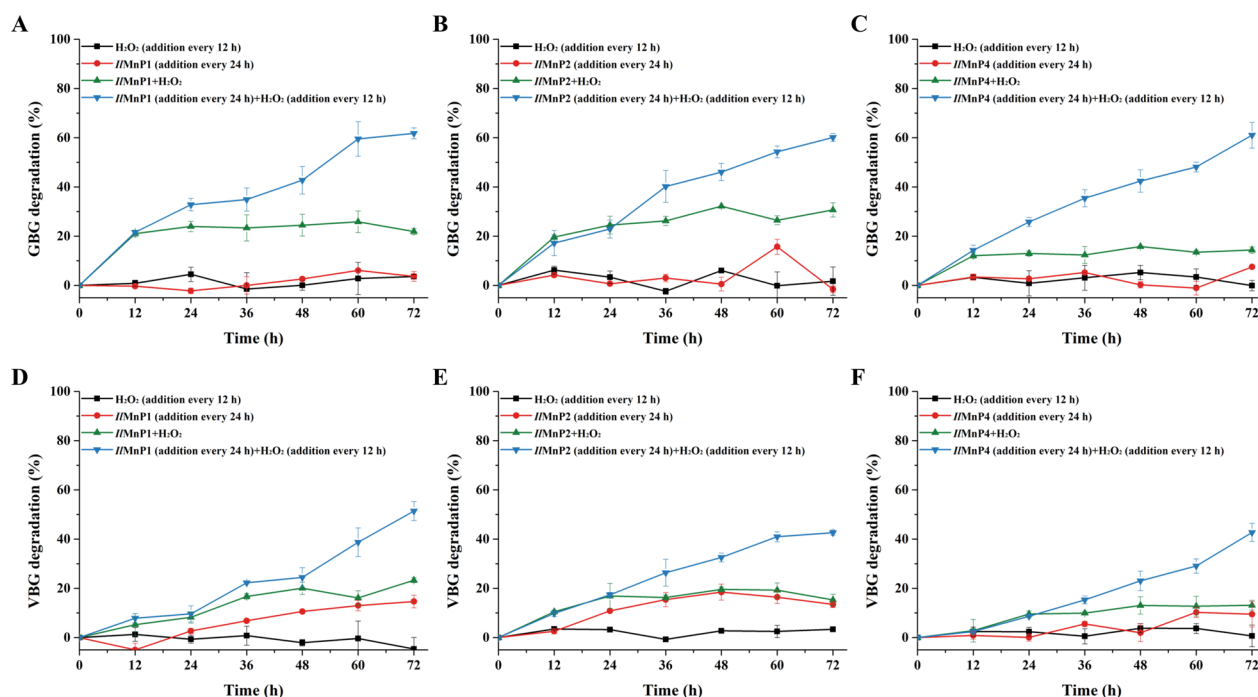


**Fig. 5** Time course analysis of the degradation ratios of dimeric lignin model compounds, the  $\beta$ -O-4 phenolic and non-phenolic lignin model dimers GBG and VBG, by purified recombinant MnPs. GBG degradation by *II*MnP1, *II*MnP2, and *II*MnP4 (A–C), and VBG degradation by *II*MnP1, *II*MnP2, and *II*MnP4 (D–F)

VBG. Based on the structure identified from the MS/MS spectrum, it was found that the  $\beta$ -O-4 phenolic and non-phenolic lignin model dimers, GBG and VBG, predominantly underwent oxidation of the hydroxyl group at  $C_\alpha$ . This process led to the formation of compounds I and III. Subsequently, the  $\beta$ -O-4 bond in compounds I and III was further cleaved, generating compounds II and IV, respectively (Fig. 6). These findings confirmed that MnP is involved in the cleavage of the  $\beta$ -O-4 bond within the lignin barrier structure, which is the most abundant inter-unit bond in the lignin barrier structure, making up 45–60% of the total lignin bonds in corn stover [36, 37].

To date, there had been quite a few reports about the oxidation and depolymerization of lignin model compounds and lignin extracted from lignocellulosic biomass by various ligninolytic enzymes in vitro, including laccase, lignin peroxidases, and dye-decolorizing peroxidases [9, 32, 38, 39]. Broadly speaking, their catalytic mechanisms underlying lignin depolymerization were relatively clear. For example, laccase was reported to oxidize  $C_\alpha$ , cleave the  $\beta$ -O-4 bond and the  $C_\alpha$ - $C_\beta$  bond in the presence of natural or synthetic mediators to achieve lignin depolymerization [40]. Lignin peroxidase and dye-decolorizing peroxidase broke down the  $C_\alpha$ - $C_\beta$  bond between lignin structural units without the help of mediators [5, 41]. In comparison to these ligninolytic enzymes, the oxidation cleavage mechanism of lignin by MnPs remained ambiguous, although MnPs had been proved to remove the lignin component of lignocellulosic biomass in vitro in the presence of the mediator unsaturated fatty acid-linoleic acid [42]. In our study, it was demonstrated that MnPs from the white rot fungus *I. lacteus* could cleave the  $\beta$ -O-4 bond in phenolic and

non-phenolic lignin model dimers without the addition of any mediator, exhibiting great application potential in the pretreatment of lignocellulosic biomass. Nonetheless, their combined effect with  $\cdot\text{OH}$  in the pretreatment of corn stover to further improve enzymatic saccharification remained to be investigated.

#### Sequential pretreatment with $\cdot\text{OH}$ and MnP for the efficient enzymatic saccharification of corn stover

To further verify the combined effect of  $\cdot\text{OH}$  and MnP pretreatment on the enzymatic saccharification of lignocellulosic biomass, a sequential pretreatment of corn stover was performed. As shown in Fig. 7A, the enzymatic saccharification of alone  $\cdot\text{OH}$ , alone MnP, and combined  $\cdot\text{OH}$  and MnP pretreated corn stover using commercial cellulase resulted in reducing sugars production of  $0.32 \pm 0.02$  mg/mL,  $0.34 \pm 0.04$  mg/mL, and  $0.63 \pm 0.04$  mg/mL, respectively, while the control without pretreatment yielded  $0.16 \pm 0.01$  mg/mL. According to the calculation, the production of reducing sugars in the  $\cdot\text{OH}$ , MnP, and combined  $\cdot\text{OH}$  and MnP pretreated groups was increased by 98%, 111%, and 290%, respectively, compared to the control group. In addition, the degree of synergy between  $\cdot\text{OH}$  and MnP pretreatment on the enzymatic saccharification of corn stover was 1.39, confirming that there were synergistic effects between  $\cdot\text{OH}$  and MnP pretreatment on the enzymatic saccharification of corn stover.

Meanwhile, in order to elucidate the mechanism underlying the synergistic action between  $\cdot\text{OH}$  and MnP on the enzymatic saccharification of corn stover, the changes in cellulose accessibility of corn stover among different pretreatment groups were evaluated. As shown in Fig. 7B, the dye adsorption ratio (DO15/

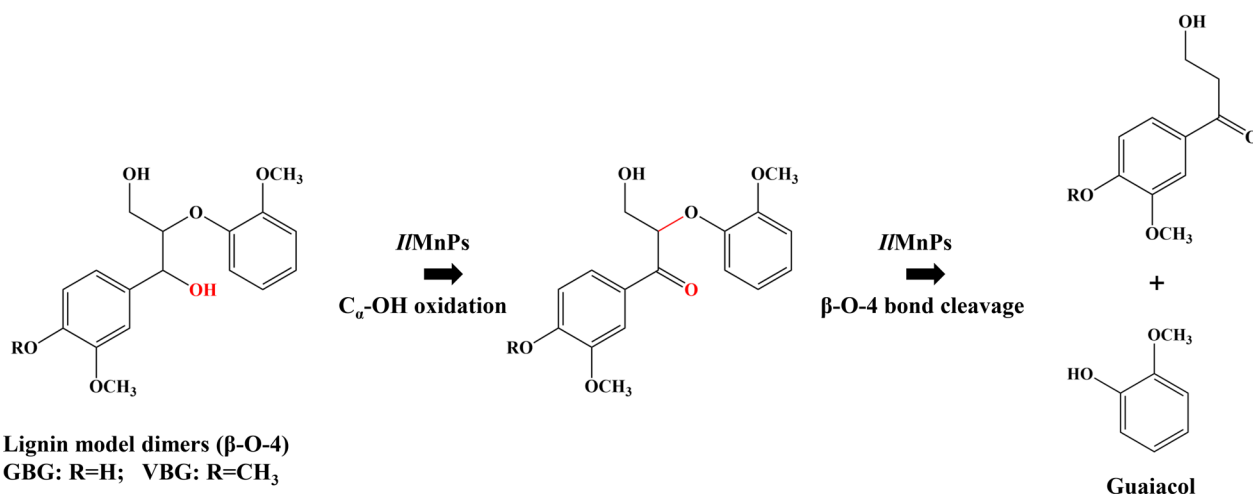


**Fig. 6** Graphic representation of the degradation process of the  $\beta$ -O-4 phenolic and non-phenolic lignin model dimers GBG and VBG by MnPs

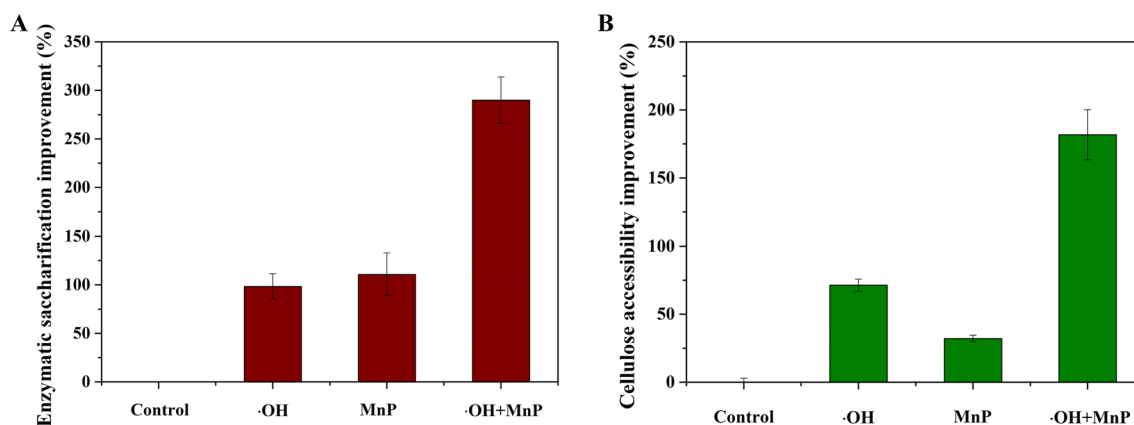


**Fig. 7** Effects of combined pretreatment with  $\cdot\text{OH}$  and MnP on the improvement of enzymatic saccharification and cellulose accessibility of corn stover. Enzymatic saccharification improvement (**A**) and cellulose accessibility improvement (**B**)

DB1), which served as an indicator of cellulose accessibility in  $\cdot\text{OH}$ , MnP, and combined  $\cdot\text{OH}$  and MnP pretreated corn stover [27], was  $1.33 \pm 0.03$ ,  $1.03 \pm 0.02$ , and  $2.19 \pm 0.14$ , respectively, compared to  $0.78 \pm 0.02$  in the control group. After calculation, the improvement in cellulose accessibility was 71%, 32%, and 182%, respectively. Furthermore, changes in the surface structure of different pretreated corn stover were consistent with the changes in cellulose accessibility (Additional file 5). These results indicated that the combined action of  $\cdot\text{OH}$  and MnP pretreatment led to a greater improvement in cellulose accessibility, making corn stover more susceptible to enzymatic saccharification by cellulolytic enzymes.

Taken together, our findings demonstrated for the first time the sequential pretreatment with  $\cdot\text{OH}$  and MnP could significantly enhance the enzymatic saccharification of corn stover. According to the variations in the enzymatic saccharification and surface structure of corn stover, it could be inferred that the preferential action of  $\cdot\text{OH}$ , a low molecular weight oxidant, could trigger the degradation of lignocellulosic biomass in cases where the ligninolytic enzymes were unable to penetrate the lignocellulosic structural barriers. Once the lignocellulosic surface structure was damaged, MnP took full advantage of this situation to come into contact with more lignin and break it down into smaller units, resulting in a significant increase in cellulose accessibility to cellulolytic enzymes. Apart from the fact that pretreatment with  $\cdot\text{OH}$  makes lignin more accessible to ligninolytic enzymes, there were still some problems to be solved. For example, the lignin-related degradation products generated by the pretreatment with  $\cdot\text{OH}$  could activate transcription factors

that modulated the expression of ligninolytic enzymes in vivo. Therefore, further studies on the interactions between reactive oxygen species and ligninolytic enzymes during the deconstruction of lignocellulosic structural barriers by white rot fungi were needed.

## Conclusion

In summary, extracellular enzyme activities and temporal secretomic analysis revealed that the  $\cdot\text{OH}$ -derived reactive oxygen species and the MnP-centered ligninolytic enzyme system were involved in the lignocellulose deconstruction by the white rot fungus *I. lacteus*. Subsequently, their function in the breakdown of lignocellulosic structural barriers was demonstrated in vitro. On the one hand,  $\cdot\text{OH}$  pretreatment could significantly enhance enzymatic saccharification by disrupting the smooth surface structure of corn stover. On the other hand, purified recombinant MnPs from *I. lacteus* were able to cleave the  $\beta\text{-O-4}$  bond in phenolic and non-phenolic lignin model dimers without the addition of any mediator. On this basis, the sequential pretreatment of corn stover with  $\cdot\text{OH}$  and MnP was carried out and showed significant synergistic effects in improving enzymatic saccharification and cellulose accessibility. Generally speaking, these findings demonstrated for the first time the great application potential of combined  $\cdot\text{OH}$  and MnP pretreatment for the efficient enzymatic saccharification of corn stover.

## Abbreviations

|                  |   |
|------------------|---|
| $\cdot\text{OH}$ | Hydroxyl radical  |
| MnP              | Manganese peroxidase                                    |
| GBG              | Guaiacylglycerol- $\beta$ -guaiacyl ether               |
| VBG              | Veratrylglycerol- $\beta$ -guaiacyl ether               |
| ABTS             | 2,2'-Azino-bis(3-ethylbenzothiazoline-6-sulphonic acid) |
| SEM              | Scanning electron microscopy                            |
| DMP              | 2,6-Dimethylphenol                                      |
| GUA              | Guaiacol  |
| RB5              | Reactive black 5  |

RB19 Reactive black 19  
DO15 Direct Orange 15  
DB1 Direct Blue 1

## Supplementary Information

The online version contains supplementary material available at <https://doi.org/10.1186/s13068-024-02583-5>.

Additional file 1. Primers used in this study.

Additional file 2. SDS-PAGE (A) and UV-visible spectroscopic (B) analysis of purified //MnPs. Lanes: M, the protein molecular mass marker; 1, 2, and 3, the purified //MnP1, //MnP2, and //MnP3, respectively.

Additional file 3. Optimum pH of purified //MnPs oxidizing different substrates, including ABTS (A), DMP (B), GUA (C), Mn<sup>2+</sup> (D), RB5 (E), and RB19 (F).

Additional file 4. UPLC-MS/MS spectrum of degradation products of GBG and VBG by purified //MnPs, including C<sub>17</sub>H<sub>18</sub>O<sub>6</sub> (A), C<sub>10</sub>H<sub>12</sub>O<sub>4</sub> (B), C<sub>18</sub>H<sub>20</sub>O<sub>6</sub> (C), and C<sub>11</sub>H<sub>14</sub>O<sub>4</sub> (D).

Additional file 5. Scanning electron microscopic analysis of corn stover after -OH and/or MnP pretreatment. Control (A), -OH pretreatment (B), MnP pretreatment (C), and -OH plus MnP pretreatment (D).

## Acknowledgements

Not applicable.

## Author contributions

MZ: investigation. YW (Yaru Wang) resources. YW (Yuan Wang): funding acquisition. TT: data curation. JZ: visualization. XW: visualization. GZ: resources. HH: data curation. BY: funding acquisition, project administration. HL: project administration, writing—review and editing. XQ: conceptualization, funding acquisition, writing—original draft. All authors read and approved the final manuscript.

## Funding

This work was supported by the National Key Research and Development Program of China (No. 2022YFD1300505), the National Natural Science Foundation of China (No. 32102583), and the China Agriculture Research System of MOF and MARA (No. CARS-41).

## Availability of data and materials

No datasets were generated or analysed during the current study.

## Declarations

### Ethics approval and consent to participate

Not applicable.

### Consent for publication

Not applicable.

### Competing interests

The authors declare no competing interests.

### Author details

<sup>1</sup>State Key Laboratory of Animal Nutrition and Feeding, Institute of Animal Science, Chinese Academy of Agricultural Sciences, Beijing 100193, China. <sup>2</sup>College of Animal Science and Technology, Ningxia University, Ningxia 750001, China.

Received: 9 September 2024 Accepted: 8 November 2024

Published online: 18 November 2024

## References

- Ashokkumar V, Venkatkarthick R, Jayashree S, Chuetor S, Dharmaraj S, Kumar G, Chen W-H, Ngamcharussrivichai C. Recent advances in lignocellulosic biomass for biofuels and value-added bioproducts—a critical review. *Biores Technol.* 2022;344: 126195.
- Mujtaba M, Fernandes Fraceto L, Fazeli M, Mukherjee S, Savassa SM, Araujo de Medeiros G, do Espírito Santo Pereira A, Mancini SD, Lipponen J, Vilaplana F. Lignocellulosic biomass from agricultural waste to the circular economy: a review with focus on biofuels, biocomposites and bioplastics. *J Clean Prod.* 2023;402: 136815.
- Sidana A, Yadav SK. Recent developments in lignocellulosic biomass pretreatment with a focus on eco-friendly, non-conventional methods. *J Clean Prod.* 2022;335: 130286.
- Yoo CG, Meng X, Pu Y, Ragauskas AJ. The critical role of lignin in lignocellulosic biomass conversion and recent pretreatment strategies: a comprehensive review. *Biores Technol.* 2020;301: 122784.
- Atiweh G, Parrish CC, Banoub J, Le TAT. Lignin degradation by microorganisms: a review. *Biotechnol Progr.* 2022;38: e3226.
- Messner K, Fackler K, Lamaipis P, Gindl W, Srebotnik E, Watanabe T. Overview of white-rot research: where we are today. In: *Wood deterioration and preservation*, vol. 845. American Chemical Society; 2003. p. 73–96.
- Sigoillot J-C, Berrin J-G, Bey M, Lesage-Meessen L, Levasseur A, Lomascolo A, Record E, Uzan-Boukhris E. Chapter 8—Fungal strategies for lignin degradation. In: *Jouanin L, Lapierre C, editors. Advances in botanical research*, vol. 61. Academic Press; 2012. p. 263–308.
- Hammel KE, Kapich AN, Jensen KA, Ryan ZC. Reactive oxygen species as agents of wood decay by fungi. *Enzyme Microb Technol.* 2002;30:445–53.
- Suryadi H, Judono JJ, Putri MR, Ecclesia AD, Ulhaq JM, Agustina DN, Sumiati T. Biodelignification of lignocellulose using ligninolytic enzymes from white-rot fungi. *Heliyon.* 2022;8: e08865.
- Bissaro B, Várnai A, Röhr ÁK, Eijsink VGH. Oxidoreductases and reactive oxygen species in conversion of lignocellulosic biomass. *Microbiol Mol Biol Rev.* 2018. <https://doi.org/10.1128/mmb.00029-00018>.
- Zhao X, Zhang L, Liu D. Biomass recalcitrance. Part II: Fundamentals of different pre-treatments to increase the enzymatic digestibility of lignocellulose. *Biofuels Bioprod Bioref.* 2012;6:561–79.
- Castaño JD, Zhang J, Anderson CE, Schilling JS. Oxidative damage control during decay of wood by brown rot fungus using oxygen radicals. *Appl Environ Microbiol.* 2018;84:e01937-e11918.
- Sheng Y, Hu J, Kukkadapu R, Guo D, Zeng Q, Dong H. Inhibition of extracellular enzyme activity by reactive oxygen species upon oxygenation of reduced iron-bearing minerals. *Environ Sci Technol.* 2023;57:3425–33.
- Qin X, Su X, Luo H, Ma R, Yao B, Ma F. Deciphering lignocellulose deconstruction by the white rot fungus *Irpex lacteus* based on genomic and transcriptomic analyses. *Biotechnol Biofuels.* 2018;11:58.
- Arantes V, Milagres AMF. The synergistic action of ligninolytic enzymes (MnP and Laccase) and Fe<sup>3+</sup>-reducing activity from white-rot fungi for degradation of Azure B. *Enzyme Microb Technol.* 2007;42:17–22.
- Aguilar A, Souza-Cruz PBD, Ferraz A. Oxalic acid, Fe<sup>3+</sup>-reduction activity and oxidative enzymes detected in culture extracts recovered from *Pinus taeda* wood chips biotreated by *Ceriporiopsis subvermispora*. *Enzyme Microb Technol.* 2006;38:873–8.
- Xu C, Ma F, Zhang X, Chen S. Biological pretreatment of corn stover by *Irpex lacteus* for enzymatic hydrolysis. *J Agric Food Chem.* 2010;58:10893–8.
- Cao X, Zuo S, Cai R, Yang F, Jiang X, Xu C. Expansion combined with *Irpex lacteus* fungal treatment for enhancing buckwheat straw degradation. *Biochem Eng J.* 2023;197: 108994.
- Niu D, Zuo S, Ren J, Huhetaoli, Zheng M, Jiang D, Xu C. Novel strategy to improve the colonizing ability of *Irpex lacteus* in non-sterile wheat straw for enhanced rumen and enzymatic digestibility. *Appl Microbiol Biotechnol.* 2020;104:1347–55.
- Ahrendt SR, Mondo SJ, Haridas S, Grigoriev IV. MycoCosm, the JGI's fungal genome portal for comparative genomic and multiomics data analyses. *Methods Mol Biol.* 2023;2605:271–91.
- Qin X, Sun X, Huang H, Bai Y, Wang Y, Luo H, Yao B, Zhang X, Su X. Oxidation of a non-phenolic lignin model compound by two *Irpex lacteus* manganese peroxidases: evidence for implication of carboxylate and radicals. *Biotechnol Biofuels.* 2017;10:103.
- Sun P, Huang Z, Banerjee S, Kadowaki MAS, Veersma RJ, Magri S, Hilgers R, Muderspach SJ, Laurent CVFP, Ludwig R, et al. AA16 oxidoreductases

- boost cellulose-active AA9 lytic polysaccharide monooxygenases from *Myceliophthora thermophila*. *ACS Catal.* 2023;13:4454–67.
23. Wiśniewski JR, Zougman A, Nagaraj N, Mann M. Universal sample preparation method for proteome analysis. *Nat Methods.* 2009;6:359–62.
  24. Tyanova S, Temu T, Cox J. The MaxQuant computational platform for mass spectrometry-based shotgun proteomics. *Nat Protoc.* 2016;11:2301–19.
  25. Martinez-D'Alto A, Yan X, Detomasi TC, Saylor RI, Thomas WC, Talbot NJ, Marletta MA. Characterization of a unique polysaccharide monooxygenase from the plant pathogen *Magnaporthe oryzae*. *Proc Natl Acad Sci.* 2023;120: e2215426120.
  26. Erabi M, Goshadrou A. Bioconversion of *Glycyrrhiza glabra* residue to ethanol by sodium carbonate pretreatment and separate hydrolysis and fermentation using *Mucor hiemalis*. *Ind Crops Prod.* 2020;152: 112537.
  27. Wiman M, Dienes D, Hansen MAT, van der Meulen T, Zacchi G, Lidén G. Cellulose accessibility determines the rate of enzymatic hydrolysis of steam-pretreated spruce. *Biores Technol.* 2012;126:208–15.
  28. Mattila H, Österman-Udd J, Mali T, Lundell T. *Basidiomycota fungi* and ROS: genomic perspective on key enzymes involved in generation and mitigation of reactive oxygen species. *Front Fungal Biol.* 2022;3: 837605.
  29. Kato DM, Elia N, Flythe M, Lynn BC. Pretreatment of lignocellulosic biomass using Fenton chemistry. *Biores Technol.* 2014;162:273–8.
  30. Jung YH, Kim HK, Park HM, Park Y-C, Park K, Seo J-H, Kim KH. Mimicking the Fenton reaction-induced wood decay by fungi for pretreatment of lignocellulose. *Biores Technol.* 2015;179:467–72.
  31. Wang F-Q, Xie H, Chen W, Wang E-T, Du F-G, Song A-D. Biological pretreatment of corn stover with ligninolytic enzyme for high efficient enzymatic hydrolysis. *Biores Technol.* 2013;144:572–8.
  32. Zhang S, Dong Z, Shi J, Yang C, Fang Y, Chen G, Chen H, Tian C. Enzymatic hydrolysis of corn stover lignin by laccase, lignin peroxidase, and manganese peroxidase. *Biores Technol.* 2022;361: 127699.
  33. Bhanghe VP, William SPMP, Sharma A, Gabhane J, Vaidya AN, Wate SR. Pretreatment of garden biomass using Fenton's reagent: influence of Fe<sup>2+</sup> and H<sub>2</sub>O<sub>2</sub> concentrations on lignocellulose degradation. *J Environ Health Sci Eng.* 2015;13:12.
  34. Askarniya Z, Sadeghi M-T, Baradaran S. Decolorization of Congo red via hydrodynamic cavitation in combination with Fenton's reagent. *Chem Eng Process Process Intensification.* 2020;150: 107874.
  35. Zhou Z, Ouyang D, Liu D, Zhao X. Oxidative pretreatment of lignocellulosic biomass for enzymatic hydrolysis: progress and challenges. *Biores Technol.* 2023;367: 128208.
  36. Fu X, Zhang J, Gu X, Yu H, Chen S. A comprehensive study of the promoting effect of manganese on white rot fungal treatment for enzymatic hydrolysis of woody and grass lignocellulose. *Biotechnol Biofuels.* 2021;14:176.
  37. Yong KJ, Wu TY. Recent advances in the application of alcohols in extracting lignin with preserved β-O-4 content from lignocellulosic biomass. *Biores Technol.* 2023;384: 129238.
  38. Zhang S, Xiao J, Wang G, Chen G. Enzymatic hydrolysis of lignin by ligninolytic enzymes and analysis of the hydrolyzed lignin products. *Biores Technol.* 2020;304: 122975.
  39. Paul M, Pandey NK, Banerjee A, Shrotri GK, Tomer P, Gazara RK, Thatoi H, Bhaskar T, Hazra S, Ghosh D. An insight into omics analysis and metabolic pathway engineering of lignin-degrading enzymes for enhanced lignin valorization. *Biores Technol.* 2023;379: 129045.
  40. Christopher LP, Yao B, Ji Y. Lignin biodegradation with laccase-mediator systems. *Front Energy Res.* 2014;2:12.
  41. Xu L, Sun J, Qaria MA, Gao L, Zhu D. Dye decoloring peroxidase structure, catalytic properties and applications: current advancement and futurity. *Catalysts.* 2021;11:955.
  42. Masarin F, Norambuena M, Ramires HO, Demuner BJ, Pavan PC, Ferraz A. Manganese peroxidase and biomimetic systems applied to in vitro lignin degradation in *Eucalyptus grandis* milled wood and kraft pulps. *J Chem Technol Biotechnol.* 2016;91:1422–30.

## Publisher's Note

Springer Nature remains neutral with regard to jurisdictional claims in published maps and institutional affiliations.